Journal of Soils and Sediments (2024) 24:3332–3349
https://doi.org/10.1007/s11368-024-03883-x

SEDIMENTS, SEC 3 • HILLSLOPE AND RIVER BASIN SEDIMENT DYNAMICS • RESEARCH ARTICLE

Quantifying pesticide-contaminated sediment sources in tropical coastal environments (Galion Bay, French West Indies)

Rémi Bizeul[1] · Olivier Cerdan[2] · Lai Ting Pak[3] · Laurence Le Callonec[4] · Sylvain Huon[5] · Pierre Sabatier[6] · Olivier Evrard[1]

Received: 23 April 2024 / Accepted: 29 July 2024 / Published online: 15 August 2024

Abstract

Purpose Over the last 60 years, intensification of soil cultivation led to an acceleration of soil erosion and sediment delivery to river systems. In Martinique, this acceleration has led to the remobilization of a toxic insecticide (i.e. chlordecone) used in the 1970s-1990s to control banana weevil. A previous study attributed this accelerated remobilization to the application of glyphosate in plantations from the 1990s onwards. To further unambiguously confirm this link, the identification of soil erosion sources supplied to coastal sediment is essential.

Methods Accordingly, sediment fingerprinting tools were adapted and applied to a coastal sediment core collected in the Galion Bay. Potential source samples (n=37) were collected across the drainage area. Along with the coastal sediment core layers, these samples were analysed for potential tracing properties. The optimal suite of tracers was then selected and introduced into an un-mixing model to quantify their contributions to coastal sediment.

Results Results showed that subsoil (i.e. soil layer < 30 cm depth) and banana plantation soil surface supply the major sources of sediment (49-78% and 12-36%, respectively) to the Galion Bay and that their contributions increased since 2000, in line with chlordecone and glyphosate fluxes.

Conclusion This evolution may be attributed to the higher sensitivity of banana plantations to erosion that may have been enhanced by the glyphosate application leaving the soil uncovered with vegetation and to the contamination of both topsoil and deep soil layers (< 30 cm) layers with chlordecone due to its vertical transfer along the soil profile and its redistribution across hillslopes.

Keywords Sediment fingerprinting · Erosion · Chlordecone transfers · Land-to-sea continuum

1 Introduction

Soil cultivation during the last 60 years has increased pressure on tropical soils (Feïss et al. 2004). The acceleration of soil erosion leads to increased sediment delivery to river systems down to the ocean, and to the transfer of associated pollutants from terrestrial to marine ecosystems. In the French West Indies (FWI), among the pollutants detected in the environment, chlordecone pollution is the most emblematic contamination issue (Cabidoche et al. 2006).

Chlordecone ($C_{10}Cl_{10}O$) is a molecule used in the composition of an organochlorine insecticide utilised in banana plantations between 1972 and 1993 in the FWI. It was applied as a white powder at the foot of banana trees to control the banana weevil. Chlordecone has also been used in Europe, the United States, Africa and Latin America. However, FWI is likely the area of the world where this substance has been the most intensively used (Devault et al. 2022). In Martinique, the cropland areas associated with a high risk of chlordecone contamination represent 40% of the cultivated surfaces (Dromard et al. 2022). To limit the risks for the population, the European Union has set a maximum chlordecone residue level of 0.1 mg kg^{-1} in food products (Official Journal of the European Union 2008).

The input of the contamination takes place when the pesticide is applied to the soil surface. Once on the surface, it may follow different pathways: it may be stored in the soil through its binding to minerals or organic matter, it may

Communicated by Simon Pulley.

Extended author information available on the last page of the article

also be degraded by bacterial activity or transported further away laterally or vertically along with water or atmospheric fluxes (Mottes et al. 2021). Because of its physico-chemical properties, chlordecone is mainly retained in the soil. This persistence of the molecule is explained by (i) its strong hydrophobicity, its low solubility in water and its strong affinity for organic matter (Cabidoche et al. 2018; Mottes et al. 2020), (ii) its sequestration in the pores of allophanic soils and (iii)) its low biodegradability due to its chemical structure (bis-homocubane), which reduces the surface area available for chemical reactions (Woignier et al. 2012). Chlordecone persistence time in soils is currently being debated, as estimations range from decades to several centuries (Cabidoche et al. 2018; Comte et al. 2022). Moreover, a recent study (Chevallier et al. 2019) demonstrated the chlordecone biodegradation capacity and identified 17 transformation products. This study highlighted the complex chlordecone degradation processes and partly explained the difficulty in estimating the chlordecone persistence time.

Furthermore, after a certain period of sequestration in soils, a pesticide can be released into the environment and thus generate a secondary contamination (Sabatier et al. 2014; Sabatier et al. 2021) of the ecosystem, which has been recently referred to as pesticide resurrection (Mottes et al. 2021). This is evidenced by the long-term presence of toxic substances in the environment although they are no longer currently used by agricultural activities. This situation is typically observed for chlordecone, which has been banned since 1993 in the FWI, although it is still found in multiple matrices currently, with high levels of contamination measured in the environment and in living organisms (Dromard et al. 2018; Méndez-Fernandez 2018). The chlordecone remobilization can be notably explained by 1) soil-to-plant transfers (Woignier et al. 2012); 2) decrease in soil organic matter content and 3) occurrence of soil erosion processes. This last chlordecone remobilization process will be the main focus of the current investigation. Indeed, based on retrospective observations from marine sediment cores, Sabatier et al. (2021) showed a drastic increase in sedimentary fluxes in the late 1990s, concomitant with the use of glyphosate as an herbicide. As the soils exposed to erosion were highly contaminated with chlordecone, this was hypothesized to have resulted in a massive remobilization of pollutants, their supply to river systems and, ultimately, to marine environments. These processes lead to a remobilization of contaminated soils and chlordecone contamination transfer along the land-to-sea continuum, thereby impacting human activities and polluting continental and marine ecosystems, whichs alter biodiversity in the coastal transition zone (Hervé et al. 2023).

In this context, the identification of soil erosion sources is essential to effectively combat the consequences of erosion on the resurgence (i.e., secondary contamination) of chlordecone. Indeed, soil particles originating from banana plantations should supply the main potential source of chlordecone contamination to river systems, although other sources (e.g., channel banks, landslides) may also provide significant quantities of sediment to river systems, while being likely depleted in chlordecone insecticide. Sediment fingerprinting may provide a relevant tool to identify the main sediment sources to river systems in tropical and cultivated catchments (Batista et al. 2019; Lima et al. 2020). By sampling soil representative of the catchment source heterogeneity, the objective is to characterize the signatures of potential erosion sources across these landscapes and to compare them with those of marine sediment in order to quantify temporal trends of sediment source contributions along the sediment core profile through the use of un-mixing models.

The Galion River catchment (Martinique, FWI) was selected to conduct the current research. This choice is supported by two main motivations : 1) its land cover is representative of that found in the agricultural zones of the FWI (where banana and sugarcane are by far the main cultivated crops); and 2) it has been equipped with a continuous catchment farming practice and river monitoring network (*Observatoire de la Pollution Agricole aux antilLEs*, OPALE). Through the use of sediment tracing tools applied to a coastal marine sediment archive, the objectives of this study are therefore 1) to quantify the temporal evolution of sediment sources to the Galion Bay, Martinique, FWI, since the 1960s and 2) to investigate the impact of these terrigenous inputs to the Galion Bay on chlordecone transfers. Furthermore, this study gives the opportunity to develop helpful tools to evaluate the respective impacts of marine and terrigenous inputs on sediment fingerprinting model output predictions.

2 Materials and methods

2.1 Study site

The Galion River catchment is located in Martinique (FWI) and drains a surface area of 45 km^2 down to its outlet flowing into the Galion Bay on the Atlantic coast. It is a typical tropical cultivated catchment of the FWI, covered by forests on the steepest upstream part (Fig. 1), and where the main crops are sugarcane and banana, occupying 23% and 42% of the cultivated catchment area in 2021, respectively (Fig. S2). The investigated catchment shows a high risk of soil chlordecone contamination, especially in its southern part. The Galion catchment is dominated by three main types of soil, namely, Andosol, Nitisol and Ferrisol (Fig. 1). They are distributed across the catchment according to an upstream-downstream

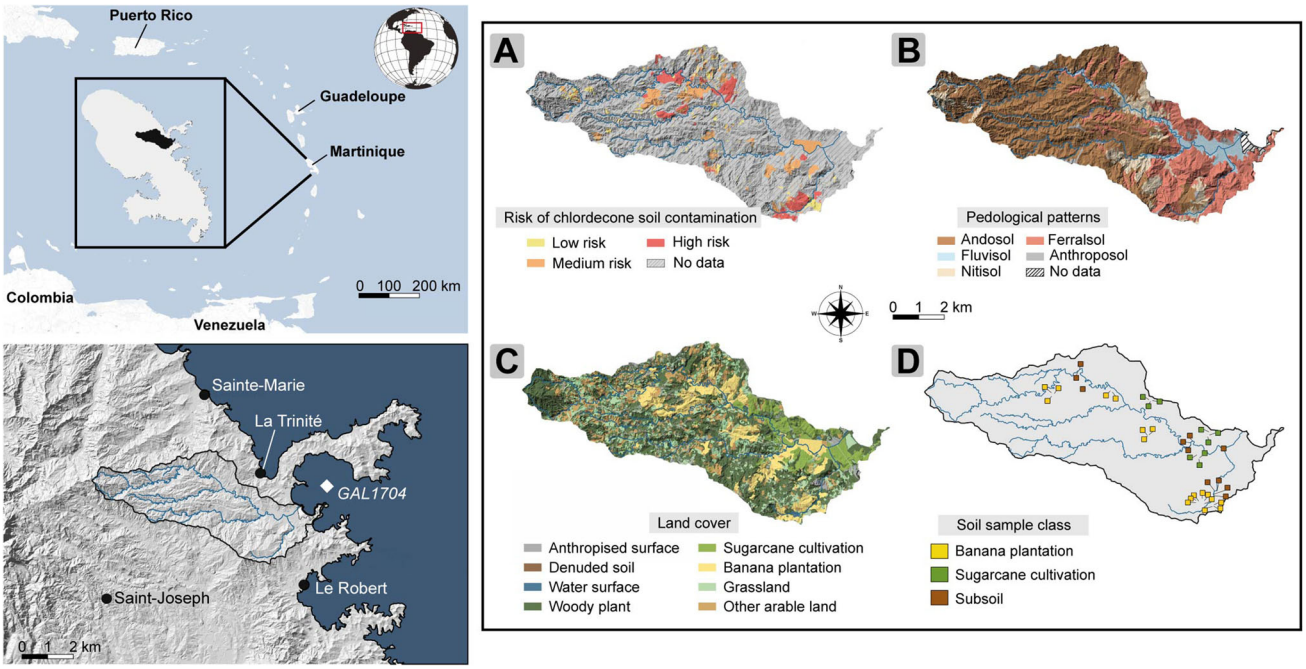

Fig. 1 Location of Martinique in Lesser Antilles, Galion catchment (position of marine sediment core GAL1704 is also defined) and A) risk of soil chlordecone contamination (BRGM), B) pedologic patterns map (source : Institut de Recherche pour le Developpement), C) land cover (source : Institut National de l'Information Géographique et Forestière, 2017) and D) location of the soil source samples (i.e. banana plantation soil surface, sugarcane crop soil surface and subsoil)

gradient. The upper catchment part is dominated by Andosol (56% of the catchment total surface). Andosol is formed by volcanic material alteration such as ash, tuff or pumice. It is a poorly developed soil composed of allophane and mineralo-organic complexes (Sierra and Desfontaines 2018). It has high aluminum, organic matter and carbon contents in addition to a high affinity with inorganic phosphate, which makes the phosphate insoluble and unavailable for uptake by plants (Baize and Girard 2008).

The middle catchment part is dominated by Nitisol (10%). As an Andosol, Nitisol was formed by volcanic material alteration. It constitutes a transitive developed soil between Andosol (poorly developed) and Ferralsol (highly developed). It shows a high organic matter and clay content. The lower part of the catchment is covered by Ferralsol (25%). The Fluviosol type is mainly found in floodplains, and it covers 6% of the catchment. The genesis and sensitivity to erosion of these contrasted soil types may differ. Nitisol usually shows lower chlordecone contents than Andosol. Nevertheless, due to its higher erosion sensitivity, Nitisol may act as a source of particle-bound transfer of chlordecone (Cabidoche et al. 2018). These differences play a major role in the contrasted sensitivity of soil types to erosion and their respective contributions to sediment and chlordecone transfers.

Catchment hydrology in tropical regions is strongly controlled by climatic fluctuations (Saffache 2000). The river regime shows very marked seasonal dynamics due to significant interannual and intraannual variability. In the FWI, there are two main seasons: a dry season from February to April, and a wet season from July to December. Due to high elevation range (0 to 694 m asl), the Galion catchment shows rainfall from 1500 mm y^{-1} in lower parts to 4000 mm y^{-1} in the upper parts (Della Rossa et al. 2017). Moreover, the marked seasonal tropical dynamics lead to strong variations in rainfall intensity throughout the year across the Galion catchment (Fig. S1). Due to these strong hydrological variations, erosion in tropical catchments is exacerbated during tropical storms. Cultivated areas are particularly sensitive to erosion processes. Based on plot monitoring and climatic modelling, Saffache (2000) estimated maximum erosion rates during extreme events of approximately 21 t ha^{-1} yr^{-1} for grassland and 39.6 t ha^{-1} yr^{-1} for croplands. Overall, this would represent 23,760 t of sediments from the Galion catchment deposited in the Galion Bay each year.

2.2 Sediment core sampling

To determine the temporal evolution of sediment sources deposited in the Galion Bay and associate chlordecone transfers, a marine sediment core was collected in April 2017 in the Galion Bay, in Martinique (Fig. 1D) (WGS84 : 14.72801600;

-60.91658800) (the sampling method is detailed in Sabatier et al. 2021). All sediment target samples were selected from this marine sediment core (n = 11). Because of its coastal sampling context, a part of the sediment may correspond to carbonate deposits in addition to the fraction of terrigenous sediment supplied to the bay by the river systems.

2.3 Soil sampling

To be as representative as possible of catchment heterogeneity (pedology, land use), a sampling scheme was designed using available GIS data (Fig. 1D). Because of the dominance of banana and sugarcane cultivation across the catchment (i.e. 42% and 23% of the total catchment cultivated area, respectively) and their expected significant contribution to sediment in the Galion Bay (Saffache 2000), land cultivated with these crop types was sampled. In addition, other sources may contribute to sediment fluxes. In the FWI, channel banks and landslides (Thiery et al. 2017) were also shown to provide significant quantities of sediment by exposing deeper soil horizons that are particularly sensitive to erosion. To take into account these erosion processes and determine the subsoil (≤ 30 cm) signature, channel banks and gullies were also sampled across the Galion catchment.

However, other potential sources may contribute to sediment fluxes. Indeed, grasslands may contribute to sediment fluxes in the Galion catchment (Saffache 2000). Nevertheless, the soil loss under this type of land cover was estimated to be lower than the three targeted sources (0.28 t ha^{-1} h^{-1} and 1.3 t ha^{-1} h^{-1}, Saffache 2000). Otherwise, although soil loss may theoretically occur in forests, soil erosion under this land use should take place with a much more limited extent than on cultivated surfaces in tropical regions (mean = 10.7 g cm^{-2} yr^{-1} and 82.5 g cm^{-2} yr^{-1} respectively, Labrière et al. 2015). For these reasons, this study focuses on the three main potential sources of erosion across the Galion catchment : soil surface under banana plantations, soil surface under sugarcane crops and subsoil (i.e. gullies, channel banks, landslides).

Soil samples were collected during two field campaigns in April 2017 and in April 2022. To determine the signature of banana plantation and sugarcane cultivation erosion sources, soil surface samples were collected from the uppermost 2 cm layer of the soil. Regarding subsoil sources (i.e. gullies, channel banks, landslides), samples were collected in areas where the deepest soil horizons were exposed to the surface. Channel banks samples were collected above the waterline. For all subsoil source samples, the sampling scheme was to collect samples at several locations within a radius of approximately 5 meters, below the area covered by the surface vegetation. Overall, soil samples were classified into three groups: 1) soil surface of banana plantations (n = 17), 2) soil surface of sugarcane crops (n = 9) and 3) subsoil (n = 11).

2.4 Sieving

Occurrence of particle size sorting during sediment transport may have an impact on fingerprint properties (Laceby et al. 2017). Indeed, fine particles with a higher specific area are generally associated with higher tracer concentrations than coarser material fractions (Collins et al. 1997). To reduce this bias, the < 63 μm fraction of soil and sediment samples was targeted and analysed in this study.

2.5 Radionuclide activities

Radionuclide activities (Bq kg^{-1}) were determined with gamma spectrometry using coaxial N- and P-type HPGe detectors at the Laboratoire des Sciences du Climat et de l'Environnement (LSCE, Gif-sur-Yvette, France). Activities ($^{210}Pb_{xs}$, ^{228}Th, ^{40}K, ^{235}U) were measured in all soil and sediment samples, and the material was packed into plastic boxes (≈ 15 g) and analyzed for 24h. The efficiency and background levels of the detectors were periodically controlled with internal and IAEA soil and sediment standards. Radionuclide activities were systematically decay-corrected to the sampling date. The marine sediment core GAL1704 was analysed for short-lived radionuclides in order to establish a core chronology. Based on $^{210}Pb_{xs}$ activity and terrigenous input proxies, an age-depth model was computed using serac R package (Bruel and Sabatier 2020). Additional information about core dating was described in Sabatier et al. (2021).

2.6 Carbon and Nitrogen isotope measurements

The removal of inorganic phases (carbonate minerals) is required before performing TOC and TN concentration and stable isotope (δ^{13}C-TOC and δ^{15}N-TN) measurements in marine sediments. Carbonate removal was conducted for selected sediment samples (n = 11), chosen for TOC and TN measurements according to their geochemical and calcimetric properties. This procedure is described in the supplementary material. Total organic carbon (TOC) and total nitrogen (TN) elemental concentrations and stable isotope ratio (δ^{13}C) were determined by the combustion method using a continuous flow elemental analyser (Elementar VarioPyro cube) coupled with an Isotope Ratios Mass Spectometer (EA-IRMS) at the Institute of Ecology and Environmental Sciences (iEES, Paris, France). Oxygen for combustion was injected for 70 s (30 mL min^{-1}) and the temperature was set at 850°C and 1120°C for the reduction and combustion furnaces, respectively (Agnihotri et al. 2014). The analytical precision was assessed with repeated analysis of a tyrosine laboratory standard (n = 49 during the course of this study), calibrated against international reference standards (Girardin and Mariotti 1991).

2.7 Elemental geochemistry

Major elemental contents (mg kg^{-1}) were determined by Energy Dispersive X-Ray Fluorescence spectrometry (Epsilon 3, Malvern Panalytical) at LSCE. Measurements were conducted on sediment and soil samples stored in air double X-ray Milar film small mass holder cells with a sample quantity between 0.8 g and 1 g. Analytical precision was assessed using the JMS-1 standard (Marine sediments from Tokyo Bay, Terashima et al. 2002). To take into account potential carbonate inputs in marine sediment, elemental geochemistry measurements were conducted on sediment before and after carbonate removal (Fig. S3, S4). Due to the difference between these two measurements and to keep the signature of the terrigenous fraction only, those properties measured after carbonate removal were chosen for incorporation in the tracer selection procedure.

2.8 Mineralogical characterization

The mineral phases found in sediment and soil samples were identified by X-Ray diffraction using a Brucker D-2 Phaser X-ray diffractometer (Cu radiation, 30 kV and 10 mA, Ni filter) at the Institut des Sciences de la Terre de Paris (ISTeP, Paris, France). The resulting spectra were analyzed using the XRD Analysis Software HighScore Plus (Malvern Panalytical) to identify the major mineral phases ($<$ 1%). Furthermore, along the sediment core, carbonate contents were determined using calcimetry measurements. This method consists of weighing 100 mg of crushed sediment and a weight range of pure $CaCO_3$ (Carlo Erba Reagents) : 10, 20, 30, 50, 75 and 100 mg for the calibration. For each sample and standard, we put powder into a sealed tube and added carefully to 2 mL of 30% HCl. We closed the tube with a barometer cap and shaken it. When HCl and powder interact, carbonate dissolution emits CO_2, which increases the pressure in the tube. This pressure is measured by the barometer-cap above the tube. The mass-pressure calibration available for the standard (10 to 100% $CaCO_3$) permits us to determine the correlation coefficient between these two properties. Finally, the carbonate content in marine sediments can be determined with the following formula :

$$\%CaCO_3 = \frac{P}{a} \quad (1)$$

where P is the measured pressure for the sample and a is the correlation coefficient obtained between pressure and weight using a $CaCO_3$ standard. These calcimetry measurements were performed to quantify the contribution of autochthonous carbonate production in sediment.

2.9 Pesticide analysis

Pesticide analyses (chlordecone, glyphosate and their respective degradation products : chlordecol and aminomethylphosphonic (AMPA)) were performed on GAL1704 core by an ALTHUS 30 ultraperformance liquid chromatography (UPLC) system (Perkin Elmer, USA) coupled in tandem to a triple quadrupole mass spectrometer equipped with an electrospray ionization (ESI) source (Perkin Elmer QSigth 200). The protocol is detailed in Sabatier et al. (2021).

2.10 Sediment source fingerprinting

To estimate the temporal evolution of sediment source contributions to Galion Bay, we applied the sediment tracing technique to the coastal marine sediment core (GAL1704). For application to sediment collected from a coastal marine environment, autochthonous carbonate production should be taken into account. Moreover, the absence of carbonate in soil has been verified in laboratory (see the procedure described in the Supplementary Material). To correct geochemical contents from this autochthonous input, X-ray fluorescence spectrometry measurements were systematically performed on decarbonateous sediment.

All subsequent processing, analyses and modeling steps were performed using the R programming environment (R Core Team 2021) within RStudio (RStudio Team 2022).

2.10.1 Tracer selection

To quantify sediment source contributions, potential tracing properties were measured in both soil and sediment samples. Before implementing a mixing model, the selection of relevant properties (tracers) was performed following the recommendations given by Chalaux-Clergue et al. (2024) and using the fingR package v.1.1.0 (Chalaux-Clergue and Bizeul 2023). The first step of this selection consisted of selecting conservative properties. The second step consisted of selecting discriminant properties. The third step led to the selection of the optimal suite of tracers using stepwise variable selection.

Conservativeness

Conservativeness evaluation consists of selecting those properties that have a distribution range similar between sources and target samples. Non-conservativeness is mainly related to two phenomena during sediment transport: particle size sorting and the occurrence of biogeochemical processes along the transport pathway and the deposition. Due to these phenomena, we must ensure that any property used to estimate sediment source contributions is not affected by transforma-

tions. This is particularly important in a coastal environment because desorption kinetics are accelerated in saline waters (Millward and Liu 2003). According to the recommendations made by Chalaux-Clergue et al. (2024), mean ± SD and hinge (i.e. interquartile range) tests were applied on merged source and target property distributions to evaluate conservativeness. A property is considered conservative when the measured values in sediment fall within the ranges of those measured in source.

Discriminant power

To evaluate the discriminating power of potential tracing properties, a two-sample Kolmogorov-Smirnov test (KS) was computed. This test compares the equality of the empirical distributions of two samples. The test hypotheses are as follows:

- H_0: Two data samples come from the same distribution.
- H_1: The distribution is statistically different between the two samples.

The KS statistic is based on the difference between empirical distributions as follows:

$$D_{n,m} = sup_x \mid F_{1,n}(x) - F_{2,m}(x) \tag{2}$$

For each pair of sources (i.e., banana plantations-subsoil; banana plantations-sugarcane crops; subsoil-sugarcane crops), this test compares the equality of the empirical distributions. The KS test was performed using the function *ks.test* from the *stats* package (R Core Team 2021).

Stepwise selection

From the selected tracers (i.e. conservative and discriminant properties), a sub-list of optimal tracers is further chosen following a stepwise variable selection. A forward stepwise variable selection based on Wilk's Lambda criterion was computed using the function *greedy.wilks* from the klaR package (Weihs et al. 2005).

2.10.2 Source modelling

To estimate sediment source contributions, the common approach (i.e. Mean Model) consists to estimate them by minimizing the sum of square residuals (SSR) of the mass balance un-mixing model (Batista et al. 2019):

$$SSR = \sum_{i=1}^{n} \left(\left(C_i - \sum_{s=1}^{m} P_s \cdot S_{si} \right) / C_i \right)^2 \tag{3}$$

which satisfies

$$\sum_{s=1}^{m} P_s = 1 \tag{4}$$

$$0 \leq P_s \leq 1 \tag{5}$$

where n is the number of elements used for modeling (i.e. tracers), C_i is the concentration of element i in the target sediment, m is the number of sources, P_s is the relative contribution of source s. However, because of $\delta^{13}C$ concentration-dependency (Phillips and Koch 2002), the current study implemented the mixing model difference (MMD) (Laceby et al. 2015; Huon et al. 2018) on $\delta^{13}C$ values:

$$MMD = \left| \left(C_r - \left(\left(\sum_{s=1}^{m} S_{sr} \cdot W_s \cdot P_{si} \right) / \left(\sum_{s=1}^{m} W_s \cdot P_{si} \right) \right) \right) / C_r \right| \tag{6}$$

where C_i is the TOC concentration in the sediment, S_{si} is the TOC (i) concentration in source, C_r is the carbon stable isotope ratio (r) in sediment, S_{sr} is the carbon stable isotope ratio (r) in source (s), W_{si} is the TOC concentration in source that is used to weight the respective carbon isotopic ratio (r), $P_s i$ is the relative contribution of source (s); and MMD is the mixing model difference that is minimized when summing absolue values and solving Eq. 6. The un-mixing model was solved by a Monte Carlo simulation with 2500 iterations using fingR package (Chalaux-Clergue and Bizeul 2023). In each iteration, target and source element concentrations were sampled from a multivariate normal distribution in order to preserve correlations between variables. Prior to modeling the multivariate distributions, element concentrations were log transformed to ensure a near normal distribution and to avoid possible negative concentration values (Batista et al. 2019).

2.10.3 Un-mixing model performance assessment

Virtual mixtures were generated to evaluate the model prediction quality. Batista et al. (2022) demonstrated that the use of virtual mixtures, compared to that of laboratory physical mixtures, provided similar results for unmixing model evaluation. Virtual source contributions were generated randomly, in the 0-100% apportionment range, with 5% increments. Virtual mixtures were generated by calculating multivariate normal distributions for the selected properties in each source group. The mean and standard deviation were calculated for each selected property and each source group to generate 138 normally-distributed samples. Then, virtual property values were generated by multiplying virtual source contributions and normally-distributed samples.

Un-mixing model were run using these virtual mixture properties. Then, the comparison of mixtures proportions computed virtually (i.e., observed contributions) and model predictions obtained when using the virtual mixtures as inputs (i.e. predicted contributions) allowed us to assess

model accuracy by calculating evaluation metrics (Matheson and Winkler 1976; Bennett et al. 2013; Batista et al. 2022) (Table S2): residual error (i.e., Mean error (ME)), performance (i.e., squared Pearson correlation coefficient (r^2), root-mean-square error (RMSE) and Nash-Sutcliffe modeling efficiency coefficient (NSE). To evaluate the multimodel contributions, the calculation of evaluation metrics was based on the mean of virtual mixture predictions obtained for both models. In addition to the calculation of evaluation metrics, a plot showing the observed versus the predicted contribution was constructed to graphically evaluate the model predictions and compare model performance in the real contribution range. These model evaluation metrics allow us to describe the model prediction quality : 1) model residuals (ME, RMSE) and 2) model performance (r^2, NSE). ME indicates the direction (over- or underestimation, shown by positive or negative ME values, respectively), while RMSE indicates the model uncertainty. The r^2 describes how linear the prediction is, and the NSE indicates the amplitude of variance explained by the model (i.e., how well the predictions match the observations). The joint use of r^2 and NSE allows a better appreciation of the distribution shape of predictions and thus facilitates the understanding of the nature of model prediction errors.

2.10.4 Model sensitivity to organic matter inputs

Due to the sensitivity of organic matter signatures to autochtonous input (marine and freshwater particular organic matter (POM), Lamb et al. 2006), terrigenous POM signal (i.e. erosion source signatures) may be disturbed. Therefore, to quantify the sensitivity of the model to greater or lower marine/terrigenous contribution, modification ratios were applied to properties measured in marine sediment samples, taking into account conservativity criteria (i.e. properties must have a similar distribution range in both source and target samples). Based on previous studies (Thornton and McManus 1994; Lamb et al. 2006), we were able to define the signature of autochtonous organic matter inputs (i.e. freshwater POM, marine POM, algae). Commonly, the comparison of δ^{13}C and TOC/TN ratio helps to determine the respective contributions of terrestrial and marine inputs of organic matter to the sediment. Therefore, four modification ratios were applied to the organic matter tracing properties (i.e. TOC and δ^{13}C) : -5%, -10% (i.e. more influence of marine POC), +5% and +10% (i.e. more influence of terrestrial input).

3 Results

3.1 Sediment and soil characterization

Marine carbonate contents decreased along the core profile, from 28% in the bottom to 17% in the upper part of the core (Fig. 2). This trend is confirmed by the mineralogical characterization of the sediment: at approximately 30 cm, there is a shift from a dominance of carbonate minerals (i.e. aragonite, calcite) in the lower part towards a dominance of minerals characteristic of continental erosion (i.e. feldspar, kaolinite, pyroxene, serpentine, gibbsite in the upper part. The sediment core variations in density showed an increasing tendency along the profile, from 0.94 g cm^{-3} in the bottom part to 1.15 g cm^{-3} in the upper part (Fig. 2). Furthermore, the granulometric spectra median (D50) decreased, from 32.1 μm at the bottom of the core to 13.2 μm in its upper part.

Regarding sediment organic matter properties, TOC content showed an increase between 59 and 35 cm, from 2.03% to 2.68%, and a second increasing phase at 11 cm from 2.10% to 2.34% (Fig. 2). TOC/TN ratio shows constant values all along the core. In contrast, δ^{13}C decreased, from -18.6‰ at 79 cm to -23.5‰ in the upper part of the profile. Sediment organic matter properties remained in the same range as those measured in subsoil and banana plantation source samples (i.e., TOC, TOC/TN and $\delta^{13}C$)(Fig. 2). Regarding sugarcane crops source samples, their signature is different from that of sediment. Overall, soil organic matter properties varied across source classes and were systematically lower for subsoil and banana plantation than for sugarcane. Indeed, the TOC values for banana plantations and subsoil vary between 1.4% and 7.7%, 0.7% and 4.4%, respectively, and between 2.9% and 6.2% for sugarcane crops. These values indicate a lower organic carbon content in the subsoil and banana plantation samples than in the sugarcane crops samples. Thus, the TOC/TN ratio shows the same tendency with values ranging in banana plantation samples between 9.9 and 13.1, between 12.5 and 15.7 in sugarcane and between 9.4 and 15.2 in subsoil samples. This tendency is even more pronounced regarding $\delta^{13}C$ values : in soil surface of sugarcane crops, they range between -13.3‰ and -15.9‰, while that in soil surface of banana plantations they range between -20.5‰ and -25.1‰ and between -19.9‰ and -27.7‰ in subsoil samples.

Elemental geochemistry characterization of sediment after carbonate removal and of potential sources can provide relevant information about sedimentary transport (Figs. S3, S4). Comparing their variations in all types of samples, many elements in sediment were found to be outside of the range measured in potential sources. Some elements, such as Mg or Al, showed higher concentrations in sediment, which indicates an enrichment during sedimentary transport (oxidation, absorption). In contrast, some properties, such as Mn or Cu, showed lower concentrations in sediment, which indicates a depletion during sedimentary transport (reduction, desorption). Overall, these differences reinforce the necessity of removing carbonate minerals prior to measurement of geochemical properties and applying consistent statistical

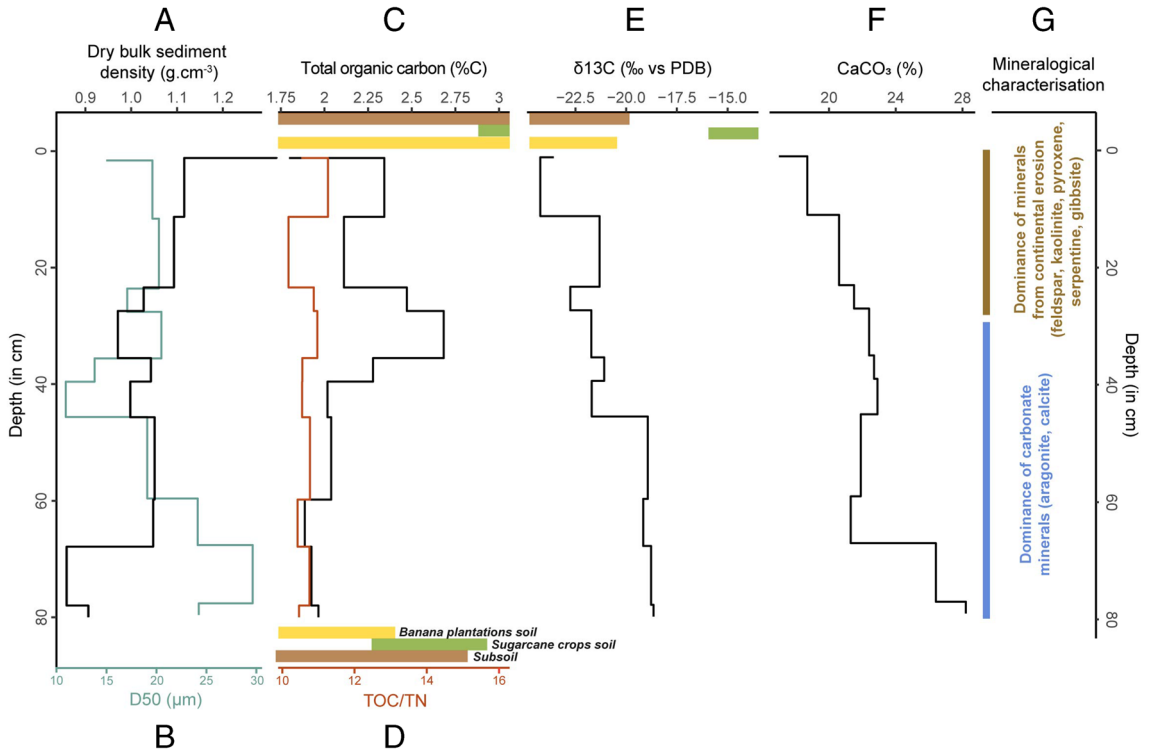

Fig. 2 Plots of core variations of A) density B) median value of granulometric spectra (D50) C) TOC D) TOC/TN E) $\delta^{13}C$ of carbonate-free samples F) $CaCO_3$ and G) mineralogical characterization. For organic matter properties (i.e. TOC, TOC/TN and $\delta^{13}C$), soil sample ranges are indicated on the top or bottom of the graphs

tests to verify the conservativity of properties as tracers along the land-to-sea continuum.

3.2 Tracer selection

Among all measured properties, five were considered conservative by statistical tests (i.e., mean ± SD and hinge tests): the three analyzed organic matter properties (TOC, TN and $\delta^{13}C$) and two geochemical properties (Ti and Cr) (Fig. 3). Among this list of properties, only TN was considered as non-discriminant by the KS test. $\delta^{13}C$ (corrected for concentration-dependency) was found to discriminate between the three source groups. Furthermore, Ti provided discrimination between banana plantation and subsoil

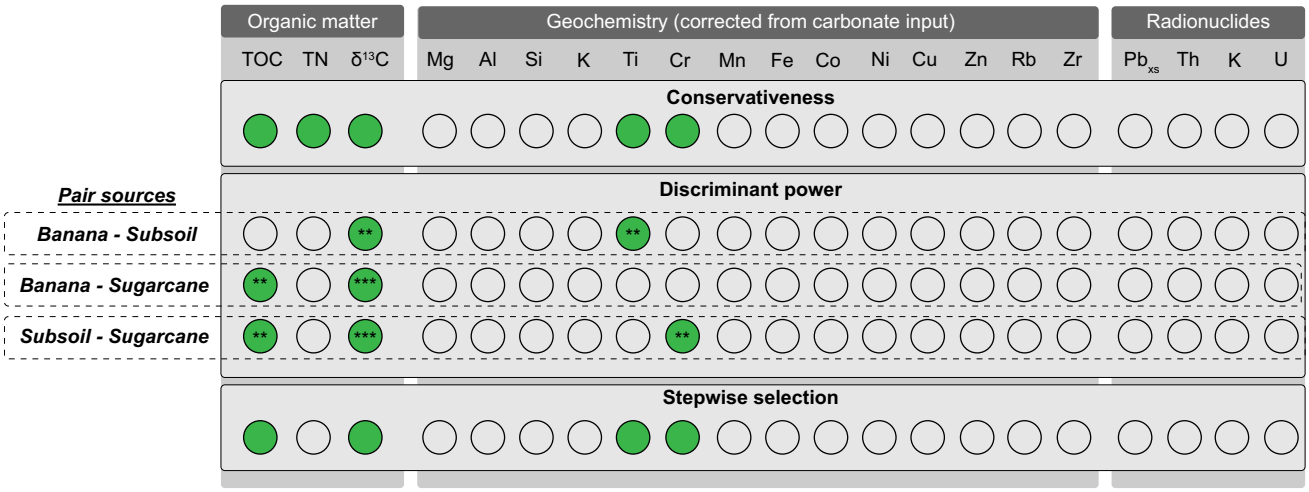

Fig. 3 Results of the tracer selection procedure. Green filled circles indicate selected properties. Significance of Kolmogorov-Smirnov (KS) test p-value : "***" p-value < 0.001; "**" p-value < 0.01

sources, TOC discriminated between banana plantation and sugarcane crops sources, and TOC and Cr differentiated between subsoil and sugarcane crops sources. Accordingly, after the evaluation of the conservativeness and discrimination power of all potential tracing properties, we obtained a list of four tracers: TOC, $\delta^{13}C$, Ti and Cr. Then, a stepwise selection was applied to this list of tracers, and all of them confirmed their relevance in tracing sources of sediment deposited in Galion Bay.

3.3 Model accuracy assessment

Regarding model residuals, ME values show that soil surface of banana plantations contribution was underestimated (ME = -0.08) by unmixing model. Banana plantations source prediction errors were higher than those for subsoil and sugarcane crops sources (RMSE = 0.20, 0.17 and 0.08 respectively). The subsoil source was better predicted than the banana plantations source but tended to be slightly overestimated (ME = 0.05). Sugarcane crops source was the best predicted (ME = -0.03) with the lowest model error (RMSE = 0.08).

Regarding model performance, sugarcane crops source prediction was highly linear (r^2=0.98) and matched well with the theoretical distributions (NSE = 0.92). As the model residuals show, the subsoil source was better predicted than the banana plantations source, and it matched better with the theoretical distribution (NSE = 0.64). However, subsoil source predictions were less linear than those of banana plantations source (r^2 = 0.76 and 0.82 respectively).

The comparison between theoretical (i.e. mixture proportions computed virtually) and predicted (i.e. model predictions obtained when using the virtual mixtures as inputs) contributions provides a graphical way to evaluate the model accuracy (Fig. 4 A,B,C). To understand how this evaluation applies to model predictions for real samples (i.e. sediment samples), the range of contributions computed for marine sediment core was also plotted on the same graph. Moreover, Chalaux-Clergue et al. (2024) highlighted that model evaluation statistics, as they are only based on virtual mixtures, are not directly transferable to actual model predictions. For this reason, a ternary diagram is also drawn (Fig. 4D), which compares contribution areas covered by theoretical, predicted and real samples. Regarding theoretical versus predicted graphs (Fig. 4 A,B,C), banana plantations contributions were likely overestimated below 23% of contribution and underestimated above this value. Along the sediment core, this means banana plantations source was overestimated in the 1950s-1970s period and in the upper part of the core (i.e. in 2016), and underestimated in the 1980s-2010s period. Subsoil contributions were underestimated below 45% of contribution and overestimated above this value. It means that subsoil contributions were underestimated throughout the entire core. However, a limited part of real subsoil contributions were not described by the virtual mixtures (for contributions > 72%). Compared to banana plantations and subsoil sources, sugarcane crops source contributions were highly linear, which is confirmed by model statistics (Table 1, r^2 = 0.98). Nevertheless, sugarcane crops source were slightly overestimated below 20% and underestimated above this value. Regarding real sample contributions, this means sugarcane crops source were slightly overestimated. Overall, sugarcane crops source contributions was slightly overestimated along the marine sediment core while banana plantations and subsoil contributions were underestimated. Nevertheless, a part of actual sample contributions were not described by virtual mixtures. This is well reflected in the ternary diagram (Fig. 4D), a part of model real predictions area ($\simeq$ 10%) lies outside of the virtual mixtures range. This divergence confirms that model evaluation metrics are not directly transferable to actual sample predictions (Chalaux-Clergue et al. 2024).

3.4 Sources of sediment inputs to Galion Bay

Based on calcimetry measurements, we can determine the proportion of sediment originating from carbonateous inputs (Fig. 5). As we have seen in Fig. 2, carbonate proportion decrease along the core from 21% in 1950s to 17% in 2016. Based on sediment core dating, the start of this decline can be attributed to the early 2000s. This relative decrease of carbonate proportion is correlated with the significant increase of terrigenous inputs during the same period, from 0.32 t ha^{-1} yr^{-1} in 1999 to 1.52 t ha^{-1} yr^{-1} in 2001.

Based on the results of the source modelling, we can identify three phases of terrigenous sediment flux, representative of the main source of sediments from the Galion catchment. Regarding banana plantations source, its contributions remained low until 1970s (< 15%) and increased during the 1980s and 1990s (28-30%). A slight increase of this source was observed during the early 2000s (+10%), synchronous to terrigenous flux increase. In the more recent part of the core (2012-2016), a slight decrease of banana plantations contribution was observed (-14%), synchronous to a slight decrease of terrigenous inputs from 1.81 t ha^{-1} yr^{-1} to 1.52 t ha^{-1} yr^{-1}.

Regarding subsoil contribution, it supplied the main source of sediment in Galion Bay along the period covered by the core. From a maximum of 74% in the 1950s, subsoil contribution decreases during the 1980s - early 2000 period (49%), in parallel to banana plantations contribution increases. During 2002-2016 period, the subsoil contributions increased again, from 49% in 2002 to 78% in 2016.

Regarding sugarcane crops contributions, it remains the source with the lowest contribution all along the core. Nev-

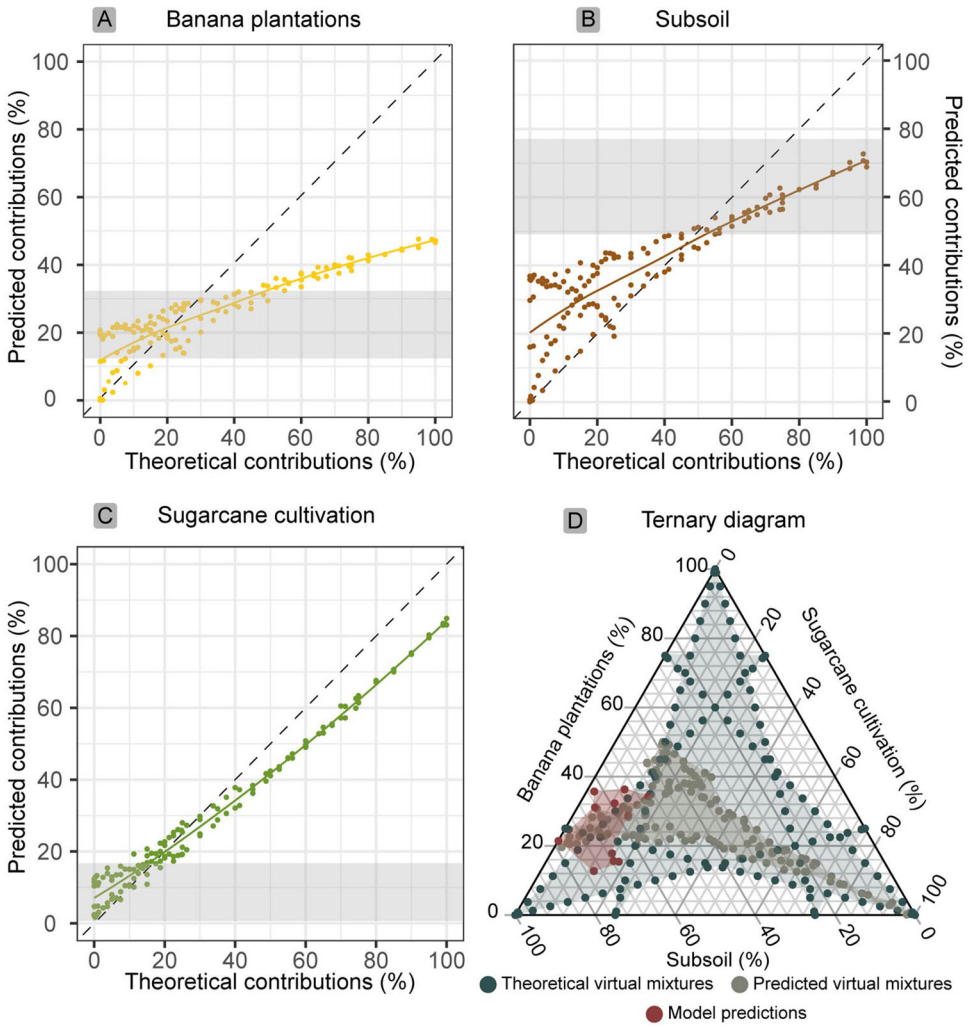

Fig. 4 Comparison between theoretical (i.e., mixture proportions computed virtually) and predicted (i.e., model predictions obtained when using the virtual mixtures as inputs) contributions for A) banana plantation, B) subsoil and C) sugarcane crops, according to the Mean Model. The grey area indicates the range of contributions computed for marine sediment core GAL1704. The dashed 1:1 line represents a perfect fit. D) The ternary plot represents contribution areas covered by theoretical virtual mixtures, predicted virtual mixtures and real samples

ertheless, significant temporal variations can be observed. During the 1950s, its contribution was equivalent to that of banana plantations (13%) and it then decreased until the early 1990s (4% in 1992). During the 1990s, the sugarcane crops contributions showed a slight increase, until the early 2000s (16% in 2002). During the 2002-2016 period, the sugarcane crops contribution decreases again down to represent only 1% of the terrigenous input in Galion Bay in 2016. Overall, based on contribution variations along the time, we can attribute the increase of sediment yield in Galion Bay since early 2000s to two sources: subsoil and soil surface of banana plantations.

Table 1 Evaluation statistics for unmixing model outputs

Sources	ME	RMSE	r2	NSE
Banana	−0.08	0.20	0.82	0.49
Subsoil	0.05	0.17	0.76	0.64
Sugarcane	−0.03	0.08	0.98	0.92

4 Discussion

4.1 Organic matter inputs to Galion Bay

4.1.1 Organic matter signatures

As mentioned above, part of the marine sediments investigated here may correspond to carbonate deposits in the water column. This autochthonous input induces a modification of the organic matter properties of the sediment. The use of the TOC/TN vs. $\delta^{13}C$ graph is widespread in the literature to determine organic matter sources (Thornton and McManus 1994; Lamb et al. 2006). In this study, organic matter properties (i.e., TN, TOC and $\delta^{13}C$) successfully contributed to the discrimination of sediment provenance (Fig. 3). Organic matter of terrestrial plants, which corresponds to plant debris, shows contrasted $\delta^{13}C$ signatures, depending on the photosynthetic pathway. The C_4 plant-type (i.e., sugarcane) shows $\delta^{13}C$ values ranging from -9‰ to -17‰, while the C_3 plants (i.e. banana tree) exhibit a range from -21‰ to -32‰ (Fig. 6).

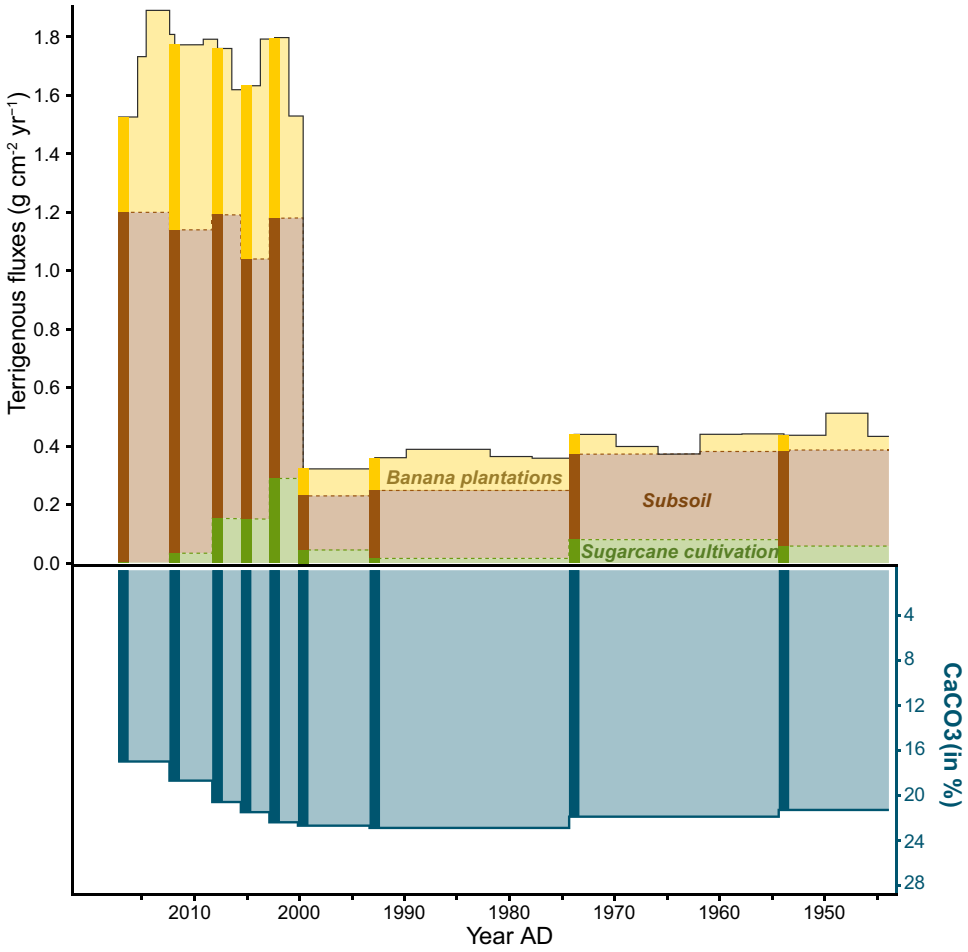

Fig. 5 Terrigenous fluxes estimated along the sediment core (Sabatier et al.) and median sediment source contributions determined using unmixing model. Carbonate contents in marine sediment are also plotted

Regarding TOC/TN ratios, terrestrial plants generally show values above 12 (Lamb et al. 2006). Nevertheless, soil organic matter may also show lower TOC/TN ratios (ca. 9), particularly for clay-rich soils, due to preferential immobilization of NH_4^+ onto clay particles (Amorim et al. 2022). The signatures of the other sources that can contribute to marine sediment, such as marine and freshwater particulate organic carbon (POC), were also plotted (Lamb et al. 2006, Fig. 6). These inputs, which are the result of autochthonous biological activity (i.e. algae, aquatic plants, bacteria), show low TOC/TN ratios (< 10) (Fig. 6) because of bacterial activities that introduce N (Rice and Hanson 1984).

To determine the main organic matter source in the Galion Bay sediment and to ensure that autochthonous biological activity did not affect the soil organic matter signal, TOC/TN and $\delta^{13}C$ values of soil and marine sediment samples were carefully examined (Fig. 6). We observed that the sediment organic matter signature corresponded mostly to that of soil under the C_3-photosynthetic pathway plant (i.e. banana tree). This confirms the dominance of soil organic matter input, mainly from soil surface of banana plantations and subsoil. The overlap between banana plantations and subsoil organic matter signatures therefore leads to model confusion and can partly explain the low model accuracy for these source predictions. At the same time, the sugarcane crops organic matter signature was more variable than that of sediment. Indeed, soil surface of sugarcane crops appears to provide a minor supply of organic matter, which remains in agreement with our model predictions (Fig. 5). Given the results of this comparison, terrigenous sources very likely provided the main source of organic matter. Otherwise, if marine organic matter origin were to be dominant, we would have observed much lower TOC/TN values (< 6 -7, Yu et al. 2010) and a greater mismatch with the terrigenous signal from soils collected across the catchment.

4.1.2 Model sensitivity to organic matter inputs

Through our additional assessment of model sensitivity to organic matter inputs, we are able to evaluate the impact of organic matter origin on model predictions (Fig. 7). By introducing negative variations (i.e. -5% and -10%) on organic matter tracing properties ($\delta^{13}C$ and TOC), we simulated a greater influence of marine POC on sediment organic matter

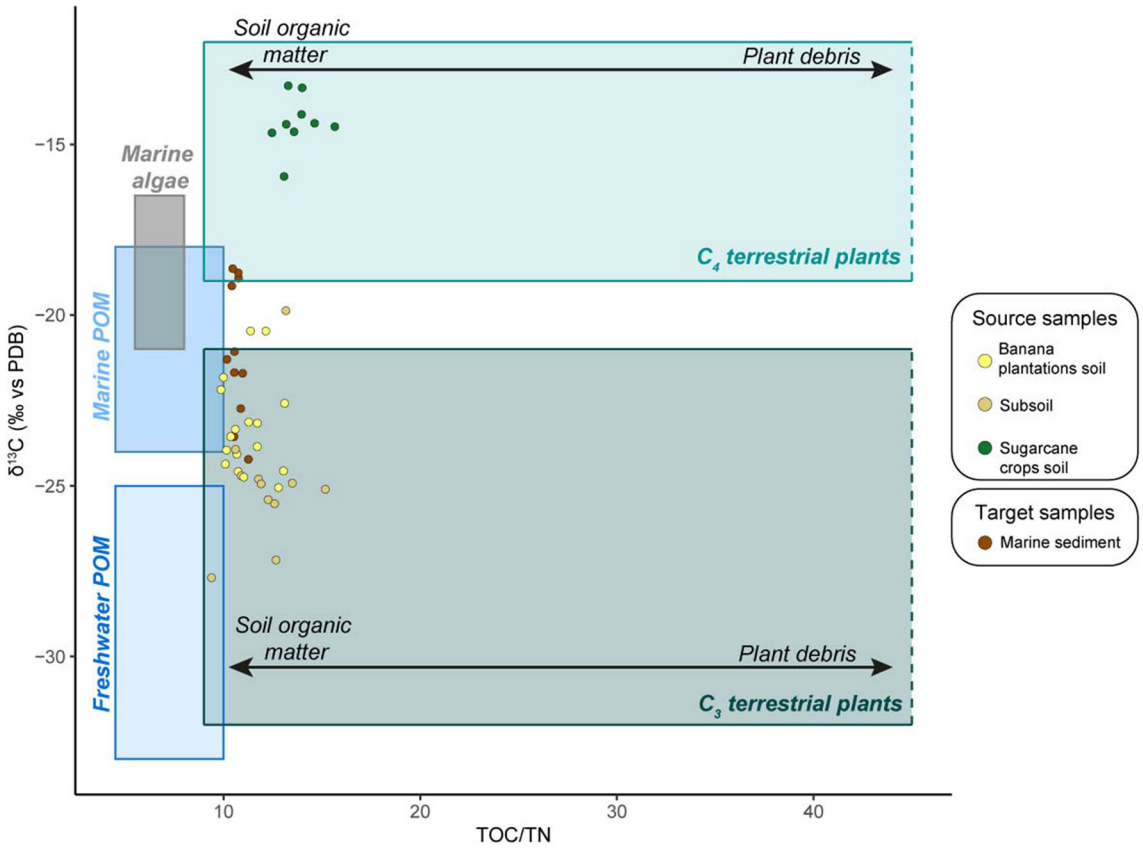

Fig. 6 $\delta^{13}C$ and TOC/TN ranges for organic inputs to coastal environments (marine and freshwater particulate organic carbon (POC)) compared to soil and sediment organic matter signatures (modified according to Lamb et al. (2006), clay-rich soil organic matter signatures (SOM) were added)

signatures (Fig. 7). It tended to reduce banana plantations contributions, by -6% and -14% in average for the -5% and -10% scenarios, respectively. This reduction was relatively constant along the core (SD = ± 2%). Conversely, subsoil and sugarcane crops contributions increased, by +4% and +2% respectively for the -5% scenario, and by +11% and +2% respectively for the -10% scenario. Overall, a greater influence of marine POC would likely have a larger impact on subsoil and banana plantations contributions, which can be explained by the closer vicinity of these two sources with the sediment organic matter signature (Fig. 6). Accordingly, any change in sediment tracing properties would have a larger impact on model predictions related to these two sources. Moreover, the wider range of the subsoil signature, due to the heterogeneity of the associated processes (i.e. river banks, gullies), likely leads the model to increase its predictions for this source when an other source contribution is reduced (banana plantation in this case). This is confirmed by the greater increase in the subsoil source compared to the sugarcane, even though the scenario considered (i.e. -5% or -10%) may bring the sediment organic matter signature closer to that of C_4 terrestrial plant signature.

By simulating an increase in organic matter tracing properties (i.e. +5% or +10%), we simulate a greater influence of terrigenous input on sediment organic matter signatures (Fig. 7). The +5% scenario has a negligible impact on model predictions (+1%, +0.3% and -1% on average for banana plantations, subsoil and sugarcane crops sources, respectively). However, the +10% scenario significantly modified model predictions by +6%, -3% and -3% on average for banana plantations, subsoil and sugarcane crops sources, respectively. Thus, simulating a greater terrigenous organic matter input leads to an increase in banana plantations contributions and a reduction of the two other source contributions. As for the -5% scenario, the impact of the -10% scenario remained constant along the core.

4.2 Geochemical signatures of erosion sources

In addition to organic matter properties, the geochemical signatures of soil and sediments provide information on the main erosion sources. Based on tracer selection tests (Fig. 3), we know that Cr discriminates soil under sugarcane crops from

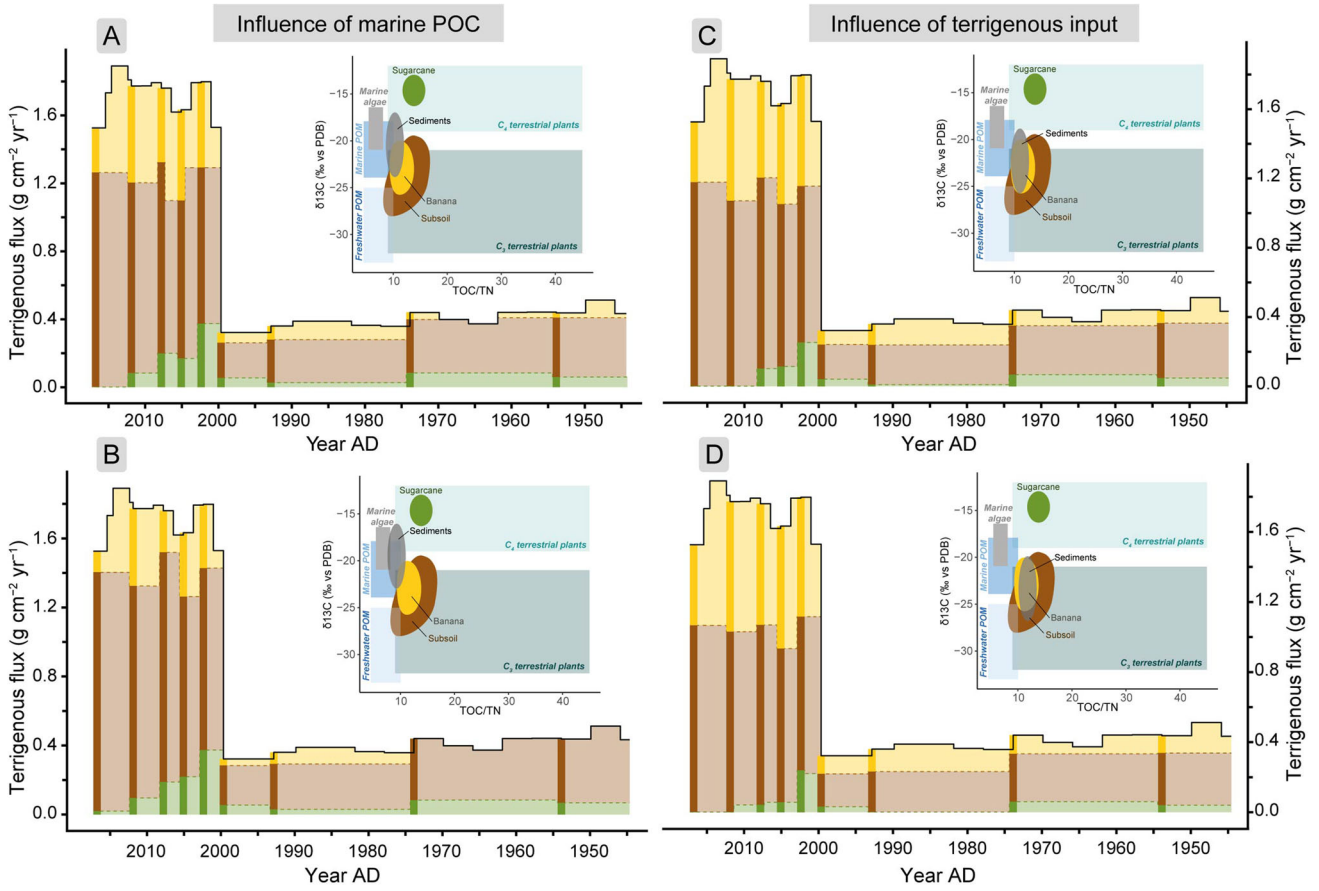

Fig. 7 Model sensitivity to organic matter inputs: influence of greater marine POC input (A -5% and B -10%) and influence of greater terrigenous input (C +5% and D +10%)

subsoil (p-value = 0.005). Indeed, Cr contents in sugarcane crops samples show a depletion compared to the two other sources (i.e., subsoil and banana plantations). This can be explained by the lower Cr contents found in Ferrisol and Nitisol (Fig. S5). Indeed, 64% and 10% of the sugarcane crops in the Galion catchment are located on Ferrisol and Nitisol, respectively.

Tracer selection tests indicate that Ti discriminates subsoil source from banana plantations source (Fig. 3, p-value = 0.002). Indeed, soil surface samples under banana plantation show a depletion in Ti contents compared to subsoil and, to a lesser extent, sugarcane crops samples (Fig. S5). The comparison of Ti contents depending on the soil type indicates that Andosols are depleted in this element compared to Ferrisol. Indeed, 50% of banana plantations in the Galion catchment are located on Andosol. This can partly explain why Ti allows the discrimination of banana plantations and subsoil sources.

Nevertheless, the use of these geochemical properties as tracers for sediment fingerprinting can be critical. Indeed, the Cr/V ratio is used in sedimentary studies as an indicator of redox conditions (Schaller et al. 1997). Moreover, Ferrisol high alteration processes (Baize and Girard 2008) and formation of Ti oxydes (i.e. titano-magnetite) can lead to an overestimation of Ti contents. Overall, these limits can partly explain the lower model prediction accuracy for subsoil and banana plantations sources, which is mostly based on geochemical properties (Table 1, Fig. 4).

4.3 Main sediment sources in Galion Bay and associated pesticides and organic carbon fluxes

4.3.1 Main sediment sources contributions

According to model estimations that are confirmed by the examination of geochemical and organic matter signatures, subsoil and soil surface of banana plantations supply the majority of sediment inputs to the Galion Bay. Moreover, the ambiguous discrimination between subsoil and banana plantations sources shown by organic matter and geochemical signatures leads to some model confusion between these two sources, as shown by the model evaluation (Table 1). Subsoil source mainly corresponds to river bank and gully erosion. These phenomena supply a significant quantity of sediment,

as shown by model predictions (Fig. 5). Gully erosion can also be observed in banana plantations of the FWI (Fig. 8A), due to their location on steep slopes and the implementation of cultivation practices sensitive to erosion (with rows parallel to the main direction of the slope (Champion 1970). In contrast, sugarcane crops, located on the flatter parts of the catchment, are better protected from gully erosion.

Moreover, the intensive ploughing practised in banana plantations results in the mixing of surface and deep soil horizons (Fig. 8B). This practice is also found in sugarcane cropland, but the flat terrain limits its impact. These two phenomena, which result from the combination of topography and agricultural practice effects, further expose the deepest horizons of banana plantation soil to erosion processes compared to sugarcane cultivation. These observations lead to the hypothesis of a double subsoil provenance: a fraction of this source likely comes from the subsurface layer of soil under banana plantations, exposed to erosion processes including gullies and deep ploughing. In contrast, the good quality of predictions of sugarcane crops contributions likely excludes the hypothesis of a significant subsurface contribution under this type of crop, not as under banana plantations.

4.3.2 Other potential sources of sediment

Nevertheless, these results need to be discussed at the light of the potential presence of sediment belonging to unattributed sources. Indeed, other sources than those three targeted in the current research may theoretically contribute to the sediment fluxes in the Galion Bay (Sec. 2.3). However, current fingerprinting tools do not allow to estimate the contribution of such unattributed sources. However, based on the literature (Saffache 2000; Labrière et al. 2015), the respective order of magnitude of soil loss under contrasted cultivated surfaces (i.e. banana plantations and sugarcane crops) is known such as that under other potential sources across the Galion catchment (i.e. grasslands and forests). Accordingly, soil loss under grassland and forest was estimated to be 5 times and 7.8 times lower, respectively, compared to that under cultivated land (Saffache 2000; Labrière et al. 2015). Sediment contributions from these sources are therefore expected to be negligible.

4.3.3 Links between source contributions, pesticides fluxes and organic carbon fluxes

Since 2000, the proportion of sediment originating from soil surface of banana plantation and subsoil increased in line with the increase in terrigenous, glyphosate and chlordecone fluxes observed in the Galion Bay (Fig. 9). As we assume that a fraction of the subsoil source may come from the deepest soil horizons of banana plantations, we therefore hypothesize that the joint increase in chlordecone fluxes occurred simultaneously with the increase in both banana plantations and subsoil contributions, which implies a chlordecone contamination in depth in banana plantations (below 30 cm). A study confirmed the hypothesis of a significant chlordecone contamination in the 30-60 cm layer, particularly in the context of deep tillage (Clostre et al. 2014). However, to the best of our knowledge, main studies about chlordecone soil contamination focused on 0-30 cm layer (Crabit et al. 2016; Comte et al. 2022). In contrast, during the same period, the proportion of sugarcane crops source decreased. This can be partly explained by the lower surface area dedicated to sugarcane cultivation in the Galion catchment since 2001 (Fig. S2).

Another assumption to explain the simultaneous increased contribution of banana plantations source contributions and the decrease in sugarcane crops source contributions

Fig. 8 Photo of A) gully in a banana plantation and B) ploughed banana plantation

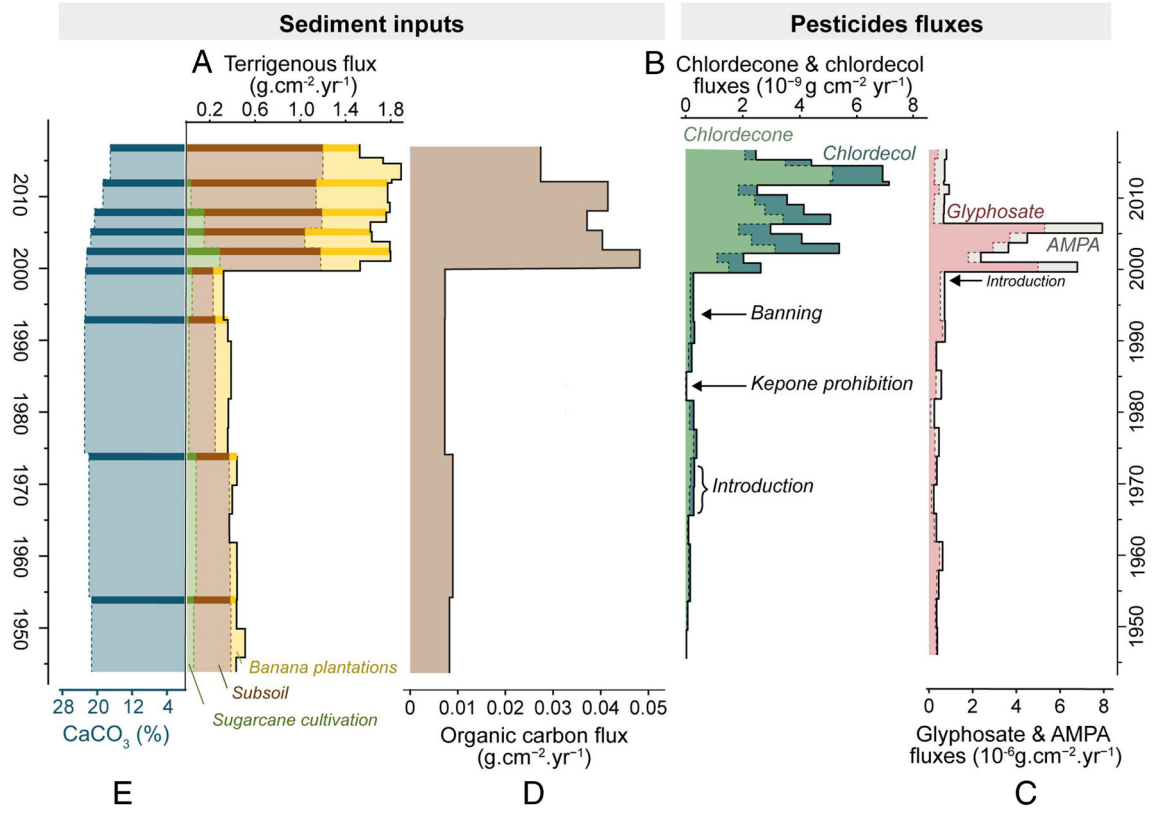

Fig. 9 A) Terrigenous fluxes, B) chlordecone and chlordecol (one of the chlordecone degradation product) fluxes, C) glyphosate and aminomethylphosphonic acid (AMPA; glyphosate degradation product) fluxes D) organic carbon fluxes and E) mean source contributions for subsoil, banana and sugarcane cultivation in successive layers of the GAL1704 marine sediment core. Pesticides (glyphosate and chlordecone) application periods are plotted on the graph as well (modified from Sabatier et al. (2021))

is the differentiated application of herbicides, especially glyphosate (Fig. 9), under these two crop types. Indeed, in the FWI, glyphosate is mostly used in banana plantations although it was not approved for sugarcane cultivation (its use is only allowed between two cultivation cycles and for paths) (DAAF, 2022). This is confirmed by the joint increase of glyphosate and aminomethylphosphonic acide (AMPA; glyphosate degradation product) and banana plantations contribution since 2000 in the Galion Bay sediment (Fig. 9). Furthermore, the link between glyphosate application and increasing soil erosion was also assumed in an recent other study (Sabatier et al. 2014).

Moreover, high sensitivity of banana plantations to soil erosion is further highlighted by the increase of banana plantation source contributions during 1980s-1990s period (Fig. 9). This increase phase is in line with the occurrence of two major tropical storms (i.e. David and Klaus). During tropical storm David, banana plantations accounted for 68% of agricultural damage in FWI (Desarthe 2014).

In addition to these increases since 2000 (i.e. terrigenous, chlordecone, glyphosate fluxes and banana plantations and subsoil contributions), organic carbon fluxes show an increasing phase (Fig. 9). It implies a large input of organic carbon to the Galion Bay. As we show that a major part of the organic matter comes from banana plantations (Fig. 6), this increase highlights the organic carbon loss with soil erosion. Furthermore, this increase in organic carbon is a major indicator of the accelerated transfer of chlordecone (i.e. resurrection) along the land-to-sea continuum since 2000. Indeed, due to the high affinity of chlordecone with organic matter, decrease in soil organic matter under banana plantations may lead to further chlordecone remobilization (Cabidoche et al. 2018).

5 Conclusion

The current research provided useful guidance for future sediment fingerprinting studies conducted in coastal tropical environments, in particular 1) the importance of relying on the pedological knowledge of the study site to support sediment source classification and 2) the power of organic matter properties to discriminate agricultural land covers (i.e. without monospecific cultivation) and 3) the support of organic matter signature to distinguish terrigenous

from marine inputs. Moreover, to the best of our knowledge, this study explicitly identified for the first time the sources of the increase in the contribution to sedimentary fluxes of surface and subsurface soil under banana plantations since 2000 in a representative catchment of the French West Indies. These phenomena can be explained by the combined effect of widespread tillage, the formation of gullies and glyphosate application under this crop type during the recent phase of agricultural intensification (i.e. since 2000). As this increase in sediment flux from both surface and subsurface sources occurs jointly with the recent increase in chlordecone fluxes, our results suggest the possible contamination of deep soil horizons (< 30 cm) with chlordecone under banana plantations. To further improve the understanding of chlordecone transfers in these environments, we suggest conducting further research to better document the distribution of chlordecone with depth in soils under banana plantations and applying sediment fingerprinting tools to suspended sediment collected in rivers draining these cultivated areas to better describe and understand the sediment and contaminant pathways in these coastal insular systems.

Supplementary Information

The dataset is available online at Bizeul et al. (2023).

Supplementary Information The online version contains supplementary material available at https://doi.org/10.1007/s11368-024-03883-x.

Acknowledgements This work was supported by Plan Chlordecone 2021-2027 (Projet SEA9- Chlordecone, Prefecture de Martinique).

Funding Open access funding provided by Commissariat à l'Énergie Atomique et aux Énergies Alternatives.

Declarations

Conflict of Interest/Competing Interests The authors have no competing interests to declare that are relevant to the content of this article.

References

Agnihotri R, Kumar R, Prasad MVSN et al (2014) Experimental setup and standardization of a continuous flow stable isotope mass spectrometer for measuring stable isotopes of carbon, nitrogen and sulfur in environmental samples. MAPAN 29(3):195–205. https://doi.org/10.1007/s12647-014-0099-8

Amorim HC, Hurtarte LC, Souza IF et al (2022) C: N ratios of bulk soils and particle-size fractions: global trends and major drivers. Geoderma 425:116026. https://doi.org/10.1016/j.geoderma.2022.116026

Baize D, Girard M (2008) Référentiel pédologique 2008. Tech. rep, AFES

Batista PVG, Laceby JP, Silva MLN et al (2019) Using pedological knowledge to improve sediment source apportionment in tropical environments. J Soils Sediments 19(9):3274–3289. https://doi.org/10.1007/s11368-018-2199-5

Batista PVG, Laceby JP, Evrard O (2022) How to evaluate sediment fingerprinting source apportionments. J Soils Sediments 22(4):1315–1328. https://doi.org/10.1007/s11368-022-03157-4

Bennett ND, Croke BF, Guariso G et al (2013) Characterising performance of environmental models. Environ Modell Softw 40:1–20. https://doi.org/10.1016/j.envsoft.2012.09.01

Bizeul R, Evrard O, Sabatier P et al (2023) Measured properties in soil samples and marine sediment collected in Galion Bay (Martinique, France) in order to trace erosion sources in insular tropical catchments [Data set]. Zenodo. https://doi.org/10.5281/zenodo.10137172

BRGM (2022) Cartographie de la contamination des sols par la chlordécone en Martinique. Tech. Rep. BRGM/RP-72061-FR

Bruel R, Sabatier P (2020) Serac: an R package for ShortlivEd RAdionuclide chronology of recent sediment cores. J Environ Radioact 225:106449. https://doi.org/10.1016/j.jenvrad.2020.106449

Cabidoche Y, Cattan P, Clermont-Dauphin C et al (2018) Pollution persistante des sols aux Antilles par des insecticides organochlorés: HCH et chlordécone encore pour des siècles ? INRA Zone Caraïbe

Cabidoche YM, Jannoyer M, Vannière H (2006) Pollution par les organochlorés aux Antilles. Tech. rep, CIRAD INRA

Chalaux-Clergue T, Bizeul R (2023) fingR: A Framework for Sediment Source Fingerprinting. Zenodo. https://doi.org/10.5281/ZENODO.8293596

Chalaux-Clergue T, Bizeul R, Batista PVG et al (2024) Sensitivity of source sediment fingerprinting to tracer selection methods. Soil 10(1):109–138. https://doi.org/10.5194/soil-10-109-2024

Champion J (1970) Les possibilités de mécanisation en culture bananière. Fruits 25(10)

Chevallier ML, Della-Negra O, Chaussonnerie S et al (2019) Natural chlordecone degradation revealed by numerous transformation products characterized in key French West Indies environmental compartments. Environ Sci Technol 53(11):6133–6143. https://doi.org/10.1021/acs.est.8b06305

Clostre F, Lesueur-Jannoyer M, Achard R et al (2014) Decision support tool for soil sampling of heterogeneous pesticide (chlordecone) pollution. Environ Sci Pollut Res 21(3):1980–1992. https://doi.org/10.1007/s11356-013-2095-x

Collins A, Walling D, Leeks G (1997) Fingerprinting the origin of fluvial suspended sediment in larger river basins: combining assessment of spatial provenance and source type. Geogr Ann 79:16

Comte I, Pradel A, Crabit A et al (2022) Long-term pollution by chlordecone of tropical volcanic soils in the French West Indies: new insights and improvement of previous predictions. Environ Pollut 119091. https://doi.org/10.1016/j.envpol.2022.119091

Crabit A, Cattan P, Colin F et al (2016) Soil and river contamination patterns of chlordecone in a tropical volcanic catchment in the French West Indies (Guadeloupe). Environ Pollut 12

Della Rossa P, Jannoyer M, Mottes C et al (2017) Linking current river pollution to historical pesticide use: insights for territorial management? Sci Total Environ 574:1232–1242. https://doi.org/10.1016/j.scitotenv.2016.07.065

Desarthe J (2014) Ouragans et submersions dans les Antilles françaises (xviie - xxe siècle). Études Caribéennes (29). https://doi.org/10.4000/etudescaribeennes.7176

Devault D, Massat F, Baylet A et al (2022) Arsenic and chlordecone contamination and decontamination toxicokinetics in Sargassum sp. Environ Sci Pollut Res 29(1):6–16. https://doi.org/10.1007/s11356-020-12127-7

Dromard C, Guéné M, Bouchon-Navaro Y et al (2018) Contamination of marine fauna by chlordecone in Guadeloupe: evidence of a seaward decreasing gradient. Environ Sci Pollut Res 25(15):14294–14301. https://doi.org/10.1007/s11356-017-8924-6

Dromard C, Devault D, Bouchon-Navaro Y et al (2022) Environmental fate of chlordecone in coastal habitats: recent studies conducted in Guadeloupe and Martinique (Lesser Antilles). Environ Sci Pollut Res 29(1):51–60. https://doi.org/10.1007/s11356-019-04661-w

Feïss C, Bonté P, Andrieu A et al (2004) Transfert de matières des bassins versants côtiers au milieu marin: identification, caractérisation et vitesse. L'exemple de la baie du Marin (Martinique). Géomorphologie: Relief Process Environ 1:81–90

Girardin C, Mariotti A (1991) Analyse isotopique du 13C en abondance naturelle dans le carbone organique: un système automatique avec robot préparateur. Cah ORSTOM, sér Pédol 26(4):371–380

Hervé V, Sabatier P, Lambourdière J et al (2023) Temporal pesticide dynamics alter specific eukaryotic taxa in a coastal transition zone. Sci Total Environ 866:161205. https://doi.org/10.1016/j.scitotenv.2022.161205

Huon S, Hayashi S, Laceby JP et al (2018) Source dynamics of radiocesium-contaminated particulate matter deposited in an agricultural water reservoir after the Fukushima nuclear accident. Sci Total Environ 612:1079–1090. https://doi.org/10.1016/j.scitotenv.2017.07.205

Labrière N, Locatelli B, Laumonier Y et al (2015) Soil erosion in the humid tropics: a systematic quantitative review. Agric Ecosyst Environ 203:127–139. https://doi.org/10.1016/j.agee.2015.01.027

Laceby JP, Olley J, Pietsch TJ et al (2015) Identifying subsoil sediment sources with carbon and nitrogen stable isotope ratios. Hydrol Process 29(8):1956–1971. https://doi.org/10.1002/hyp.1031

Laceby JP, Evrard O, Smith HG et al (2017) The challenges and opportunities of addressing particle size effects in sediment source fingerprinting: a review. Earth Sci Rev 169:85–103. https://doi.org/10.1016/j.earscirev.2017.04.009

Lamb AL, Wilson GP, Leng MJ (2006) A review of coastal palaeoclimate and relative sea-level reconstructions using δ13C and C/N ratios in organic material. Earth Sci Rev 75(1–4):29–57. https://doi.org/10.1016/j.earscirev.2005.10.003

Lima PLT, Silva MLN, Quinton J et al (2020) Tracing the origin of reservoir sediments using magnetic properties in Southeastern Brazil. Semina Cienc Agrar 41(3):847. https://doi.org/10.5433/1679-0359.2020v41n3p847

Matheson JE, Winkler RL (1976) Scoring rules for continuous probability distributions. Manage Sci 22(10):1087–1096. https://doi.org/10.1287/mnsc.22.10.1087

Méndez-Fernandez P (2018) From banana fields to the deep blue_ Assessment of chlordecone contamination of oceanic cetaceans in the eastern Caribbean. Mar Pollut Bull 5

Millward G, Liu Y (2003) Modelling metal desorption kinetics in estuaries. Sci Total Environ 314–316:613–623. https://doi.org/10.1016/S0048-9697(03)00077-9

Mottes C, Deffontaines L, Charlier J et al (2020) Spatio-temporal variability of water pollution by chlordecone at the watershed scale: What insights for the management of polluted territories? Environ Sci Pollut Res 27(33):40999–41013. https://doi.org/10.1007/s11356-019-06247-y

Mottes C, Sabatier P, Evrard P et al (2021) Pesticide resurrection. Environ Chem pp s10311–021–01347–z. https://doi.org/10.1007/s10311-021-01347-z

Official Journal of the European Union (2008) Commission of the European communities, Commission regulation (EC) No 839/2008 of 31 July 2008 amending Regulation (EC) No 396/2005 of the European Parliament and of the Council as regards Annexes II, III and IV on maximum residue levels of pesticides in or on certain products

Phillips DL, Koch PL (2002) Incorporating concentration dependence in stable isotope mixing models. Oecologia 130(1):114–125. https://doi.org/10.1007/s004420100786

R Core Team (2021) R: A Language and Environment for Statistical Computing. R Foundation for Statistical Computing, Vienna, Austria, https://www.R-project.org/

Rice DL, Hanson RB (1984) A kinetic model for detritus nitrogen: role of the associated bacteria in nitrogen accumulation. Bull Mar Sci 35

RStudio Team (2022) RStudio: Integrated Development Environment for R. RStudio, PBC, Boston, MA. http://www.rstudio.com/, version 2022.7.1.554

Sabatier P, Poulenard J, Fanget B et al (2014) Long-term relationships among pesticide applications, mobility, and soil erosion in a vineyard watershed. Proc Natl Acad Sci 111(44):15647–15652. https://doi.org/10.1073/pnas.1411512111

Sabatier P, Mottes C, Cottin N et al (2021) Evidence of chlordecone resurrection by glyphosate in French West Indies. Environ Sci Technol 55(4):2296–2306. https://doi.org/10.1021/acs.est.0c05207

Saffache P (2000) Érosion des bassins-versants et engraissement côtier: le cas de la baie du Galion (Martinique). CR Acad Sci, Ser IIa: Sci Terre Planets 330(6):423–428. https://doi.org/10.1016/S1251-8050(00)00154-3

Schaller T, Moor HC, Wehrli B (1997) Sedimentary profiles of Fe, Mn, V, Cr. As and Mo as indicators of benthic redox conditions in Baldeggersee, Aquat Sci

Sierra J, Desfontaines L (2018) Les sols de la Guadeloupe: Genèse, distribution & propriétés. INRA, Tech. rep

Terashima S, Imai N, Taniguchi M et al (2002) The Preparation and Preliminary Characterisation of Four New Geological Survey of Japan Geochemical Reference Materials: Soils, JSO-1 and JSO-2; and Marine Sediments, JMS-1 and JMS-2. Geostand Geoanal Res 26(1):85–94. https://doi.org/10.1111/j.1751-908X.2002.tb00626.x

Thiery Y, Reninger PA, Lacquement F et al (2017) Analysis of slope sensitivity to landslides by a transdisciplinary approach in the framework of future development: the case of La Trinité in Martinique (French West Indies). Geosci 7(4):135. https://doi.org/10.3390/geosciences7040135

Thornton S, McManus J (1994) Application of organic carbon and nitrogen stable isotope and C/N ratios as source indicators of organic matter provenance in estuarine systems: evidence from the Tay Estuary, Scotland. Estuarine Coastal Shelf Sci 38(3):219–233. https://doi.org/10.1006/ecss.1994.1015

Weihs C, Ligges U, Luebke K et al (2005) klar analyzing german business cycles. In: Baier D, Decker R, Schmidt-Thieme L (eds) Data analysis and decision support. Springer-Verlag, Berlin, pp 335–343, r package version 1.7.1

Woignier T, Clostre F, Macarie H et al (2012) Chlordecone retention in

the fractal structure of volcanic clay. J Hazard Mater 241–242:224–230. https://doi.org/10.1016/j.jhazmat.2012.09.034

Yu F, Zong Y, Lloyd JM et al (2010) Bulk organic δ13C and C/N as indicators for sediment sources in the Pearl River delta and estuary, southern China. Estuarine Coastal Shelf Sci 87(4):618–630. https://doi.org/10.1016/j.ecss.2010.02.018

Authors and Affiliations

Rémi Bizeul[1] · Olivier Cerdan[2] · Lai Ting Pak[3] · Laurence Le Callonec[4] · Sylvain Huon[5] · Pierre Sabatier[6] · Olivier Evrard[1]

✉ Rémi Bizeul
remi.bizeul@lsce.ipsl.fr

[1] Laboratoire des Sciences du Climat et de l'Environnement (LSCE-IPSL), Université Paris-Saclay, Unité Mixte de Recherche 8212 (CEA/CNRS/UVSQ), Orme des Merisiers, Gif-Sur-Yvette 91191, France

[2] Risk and Prevention Division, Bureau de Recherches Géologiques et Minières (BRGM), 3 av. Claude Guillemin, BP 6009, Orléans 45060, France

[3] UPR HortSys, Cirad, Petit Morne, BP 214, Le Lamentin, Martinique 97285, France

[4] Sorbonne Université, Institut des Sciences de la Terre de Paris, ISTeP, 4 place Jussieu, Paris 75005, France

[5] Sorbonne Université, Institut d'Ecologie et des Sciences de l'Environnement de Paris, 4 place Jussieu, Paris 75005, France

[6] Environnements, Dynamiques et Territoires de Montagne (EDYTEM), Université Savoie Mont Blanc, CNRS, Le Bourget du Lac 73376, France